



**HAL**  
open science

## Preparation of a novel composite based polyester nonwovens with high mechanical resistance and wash fastness properties

Ahmed Abed, Nabil Bouazizi, Stéphane Giraud, Ahmida El Achari, Christine Campagne, Olivier Thoumire, Reddad El Moznine, Omar Cherkaoui, Julien Vieillard, Abdelkrim Azzouz

### ► To cite this version:

Ahmed Abed, Nabil Bouazizi, Stéphane Giraud, Ahmida El Achari, Christine Campagne, et al.. Preparation of a novel composite based polyester nonwovens with high mechanical resistance and wash fastness properties. *Colloids and Surfaces A: Physicochemical and Engineering Aspects*, 2019, 577, pp.604-612. 10.1016/j.colsurfa.2019.05.090 . hal-02330553

**HAL Id: hal-02330553**

**<https://normandie-univ.hal.science/hal-02330553>**

Submitted on 25 Oct 2021

**HAL** is a multi-disciplinary open access archive for the deposit and dissemination of scientific research documents, whether they are published or not. The documents may come from teaching and research institutions in France or abroad, or from public or private research centers.

L'archive ouverte pluridisciplinaire **HAL**, est destinée au dépôt et à la diffusion de documents scientifiques de niveau recherche, publiés ou non, émanant des établissements d'enseignement et de recherche français ou étrangers, des laboratoires publics ou privés.



Distributed under a Creative Commons Attribution - NonCommercial 4.0 International License

## Preparation of a novel composites based polyester nonwovens with high mechanical resistance and wash fastness properties

Ahmed Abed<sup>a, b, c</sup>, Nabil Bouazizi<sup>a\*</sup>, Stéphane Giraud<sup>a</sup>, Ahmida El Achari<sup>a</sup>, Christine Campagne<sup>a</sup>, Olivier Thoumire<sup>d</sup>, Reddad El Moznine<sup>b</sup>, Omar Cherkaoui<sup>c</sup>, Julien Vieillard<sup>e</sup>, Abdelkrim Azzouz<sup>e</sup>

<sup>a</sup> ENSAIT, GEMTEX – Laboratoire de Génie et Matériaux Textiles, F-59000 Lille, France

<sup>b</sup>Laboratory LPMC, Faculty of Science El Jadida, Chouaib Doukkali University, El Jadida, Morocco.

<sup>c</sup>Laboratory REMTEX, ESITH, Route d'El Jadida, km 8, BP 7731 – Oulfa, Casablanca, Morocco

<sup>d</sup> Normandie Univ., UNIROUEN, CNRS, PBS (UMR 6270), 55 rue Saint Germain, 27000 Evreux, France

<sup>e</sup> Normandie Univ., UNIROUEN, INSA Rouen, CNRS, COBRA (UMR 6014), 55 rue Saint Germain, 27000 Evreux, France

\*CORRESPONDING AUTHOR. Dr. Bouazizi Nabil, E-mail addresses:  
[bouazizi.nabil@hotmail.fr](mailto:bouazizi.nabil@hotmail.fr)

### Abstract

In this work, polyester fiber were functionalized by oxides (Ox) like titanium dioxide (TiO<sub>2</sub>), zinc oxide (ZnO) and silicon oxide (SiO<sub>2</sub>), using polyvinylidene fluoride (PVDF) as binder to obtain the PET-PVDF-Ox samples. Chitosan polymer (CT) was coated on last samples to ensure the good surface compatibility, resulting in the PET-PVDF-Ox-CT composite. The obtained products were thermally pressed and fully characterized. The chemical coatings, physical and thermal properties were investigated. It was found that coated PET nonwoven is highly hydrophobic materials with good diffusion resistance. Incorporation of TiO<sub>2</sub>, ZnO and SiO<sub>2</sub> resulted in the formation of strong cross-linked CT network, producing improved dripping resistance of PET nonwoven. In addition, the modification steps allows to highly increasing the mechanical resistance. This was explained by the good surface compatibly and the interfacial bonding occurred in the matrix. Moreover, soil release tests confirmed the high durability against washing for PET-PVDF-Ox-CT composites. Thus,

regarding to the above results, the current work developed a facile process for the fabrication of new composite based nonwovens with good durability and high mechanical resistance.

**Keywords:** Polyester Fiber; Chitosan; PVDF; Oxides; Mechanical resistance; Durability

## 1. Introduction

Textiles have increased significantly their specific and high performance applications. One of the main fields of application for these materials is the construction industry. Textile surface produced by nonwoven technology provides a way to impart new and diverse properties like self-decontamination, hydrophilicity, hydrophobicity, retaining comfort and mechanical strength [1]. The nonwovens fabrics are fibrous structures with randomly oriented fibers, presenting important properties and characteristics to be used in different kind of applications. Hence, the increasing interest for the personal health and comfort has created the necessity to improve the mechanical properties of nonwovens. Nonwovens surface modification was considered an interesting way to enhance the properties. Therefore, value addition to PET nonwovens by functionalization produced considerable industrial attention, attributed to their potential use in physical, thermal, biological and medical protection. The outstanding mechanical character of composites is a result of the load transfer from polymer matrix to filler materials that are of higher stiffness and failure strength [2]. Thus, composite with a good tensile modulus, that target ideal mechanical strength are strongly requested [3]. It was found that the composites reinforced with chemical treatments such as the incorporation of metallic nanoparticle, the grafting of organics moieties can increase the tensile modulus. However, the chemical modifications for many works were not sufficient to produce composites with stable structure, due to the local buckling behaviors occurring during the preparation. In addition, the composites are not sustainable with heterogeneous contents with low thermal stability. There, the functionalization and fabrication of composite materials are quite required to resolve the above problems.

Up to now, the oxides (Ox), such as metallic oxide [2] and their included hydroxyl groups showed that nonwovens can produce water vapor at high temperatures through decomposition reactions [3, 4]. On the other hand, the incorporation of Ox was used as elements for mechanical resistance, which can also increase the stress tensile [5]. Materials oxides have received considerable attention in several environmental applications, as it have many interesting properties that combined the mechanical, electrical, optical and biological properties [6]. Among them, zinc oxide (ZnO), titanium dioxide (TiO<sub>2</sub>) and silicon dioxide (SiO<sub>2</sub>) are widely studied in many aspects and were the most efficient candidates due to their important application mechanical resistance, transparent electronics, varistors, surface acoustic wave devices, piezoelectric transducers and solar cells [7]. The modification with organic substance makes great contribution to the dispersion of fillers and its strengthened barrier effect properties.

Intensive researches have been focused on developing advanced nanocomposites with improved surface properties by using oxides [8]. In this regard, many oxide types were activated and modified by the addition of some active agent such as amine derivate for enhancing mechanical, electrical and sensing properties or polyvinylidene fluoride (PVDF) [9]. Due to the excellent mechanical, chemical and ecofriendly properties, polyvinylidene fluoride were widely used in various advanced applications like mechanical resistance. Nanocomposites based PVDF and oxide provided high thermal stability, mechanical properties, and impact resistance [10]. This was explained by the presence of PVDF which incorporate Ox, but also by the possible crosslink with the material [11]. In this aim, researchers have employed some natural polymers as chitosan which show many advantages over artificial materials [12, 13]. Recently, the chitosan was established as a good candidate in total biodegradability, non-toxicity and fiber formation properties [14-16]. Indeed, the chitosan can improve the mechanical properties when optimizing particle distribution and

surface compatibility [16]. To the best of our knowledge, studies relating a combination chitosan and PVDF additives have not been reported.

On the basis of the above ideas, polyester nonwovens (PET) were employed for the fixation of Ox like TiO<sub>2</sub>, ZnO and SiO<sub>2</sub>, with the presence of poly (vinylidene fluoride) (PVDF) as binder. Then, chitosan (CT) was employed as natural polymer to reinforce the immobilization of PVDF-Ox into nonwovens fibers. The obtained materials PET-PVDF-Ox-CT were used as sustainable materials to increase the, mechanical resistance, and wash fastness properties improvements. Different modified nonwoven were systematically characterized by field emission scanning electron microscopy (SEM), optical microscopy, Fourier transform infrared (FT-IR) spectroscopy, thermogravimetric analysis (TGA), and water contact angle. The surface compatibility and the changes of mechanical, properties were investigated on the basis of the materials structure, stability and the reusability.

## **2. Experiments**

### **2.1. Materials**

Poly (vinylidene fluoride) (PVDF), inorganic nanoparticles ZnO and TiO<sub>2</sub> were purchased from Sigma-Aldrich. SiO<sub>2</sub> nanoparticles were synthesized by sol gel synthesis and the protocol is described in supporting file. Acetone and N, N-dimethylformamide (DMF), ethanol, sodium triphosphate (PPT), distilled water, ammonia hydroxide (NH<sub>4</sub>OH, NH<sub>3</sub> basis), sodium hydroxide (NaOH) and tetraethoxysilane (TEOS) were obtained and used as obtained. Polyester nonwovens (PET) with 0.9µm fiber diameter were obtained from CETI (supporting information).

### **2.2. Preparation and design of composite based nonwovens**

**Scheme. 1** illustrates the preparation and design route employed for nonwoven composite. The process mainly consisted of the following steps:

Firstly, in order to remove impurities and spinning oil present on the surface, the polyester (PET) nonwoven was treated according our previously published work [16]. Briefly, PET was

activated by air atmospheric plasma to introduce both –OH and –COOH groups at the fiber surface (**supporting information**). Secondly, three solutions were prepared, containing different oxides (i.e. TiO<sub>2</sub>, ZnO or SiO<sub>2</sub>) and PVDF as reagents with a weight ratio (3:5) and mixture of acetone and DMF (45:5 v/v) as solvent. The resulting solution was stirred for 2 h at 50 °C. After that, at room temperature, PET nonwovens were impregnated into the dispersed solution for 2 hours. The coated nonwovens were taken out from the solution and dried in at 50 °C for 24 h to clean and remove residual solvent in the resulting PET-PVDF-TiO<sub>2</sub>, PET-PVDF-SiO<sub>2</sub>, and PET-PVDF-ZnO composites. Thirdly, each composite (i.e. **PET-PVDF-Ox**) was prone to the chemical grafting of chitosan (CT) by padding with an aqueous solution of 3 g/L chitosan polymer in presence of sodium triphosphate (PPT). The fabric was then dried (110 °C, 3 min) and cured (170 °C, 30 s) using a hot air dryer (Werner Mathis AG, Switzerland). Finally the obtained products denoted PET-PVDF-Ox-CT was hot-pressed before further characterization and tests.

..... (Scheme.1) .....

### **2.3. Characterizations**

The treated and original PET nonwovens were fully characterized in this work. Fourier transform IR spectroscopy was carried out using a Tensor 27 (Bruker) spectrometer with a ZnSe ATR crystal. The samples were analyzed by FTIR directly without any further preparation, and background spectra were recorded on air. For field emission scanning electron microscopy (SEM) using a JEOL JEM-ARM200F HR setting with a field emission gun and probe aberration corrector, materials were previously metallized by a gold layer at 18 mA for 360 s with a Biorad E5200 device, and EDX images to evaluate the chemical contrast. Thermal analysis **was performed** by thermo gravimetric analysis (TG-DTA, A6300R). The water contact angle measurements were carried out by using Digidrop device from GBX. This

instrument uses a goniometric method to calculate the contact angle between water and a solid surface.

#### **2.4. Wash fastness and durability tests**

Washing process was performed by using the AATCC standardization for home laundry test [27] and can be summarized briefly as follows: 2 g of  $\text{Na}_2\text{CO}_3$  and 1 g of commercial detergent were both dissolved in one liter (1L) washing solution. Droplets of sunflower oil are deposited on unmodified and modified nonwovens PET, PET-PVDF- $\text{TiO}_2$ -CT, PET-PVDF- $\text{SiO}_2$ -CT and PET-PVDF- $\text{ZnO}$ -CT, then all samples were completely immersed in the washing solution using 1:50 material to liquor ratio at  $40^\circ\text{C}$  for 60 min, under continuous stirring. After that, nonwoven composites were removed from solution, and then rinsed with tap water until neutralization. Finally, the samples were dried in oven at  $70^\circ\text{C}$  and this process was repeated 3 times.

#### **2.5. Mechanical measurements**

Before the measurements of mechanicals properties, all materials were subjected to a hot press for 5 minutes at  $120^\circ\text{C}$  between two metal metals. The mechanical properties were of great importance to evaluate the strength of the as-prepared composite. For this, mechanical tests of all samples were carried out using MTS (2/M) testing system. According to the test procedure ISO 9073-3, each composite was cut in  $20 \times 5 \text{ cm}^2$  (L, l) size and then the measurements of tensile strength were obtained.

### **3. Results and Discussions**

#### **3.1. Role of thermal pressure**

The thermal pressure employed for the prepared composite PET-PVDF-Ox-CT in this work was an interesting step for both the construction and the tailoring of the surface compatibility of the finished materials. During the thermal pressure, the particles of Ox were connected the one to the other and compacted, due to the increases in the strong crosslink at

the particle-particle contact. The thermal pressure causes the breaking of the TiO<sub>2</sub>, SiO<sub>2</sub> and ZnO, layers on the PET fibers surfaces, resulting in direct metal to fiber contacts. In this situation, the process improves the crosslink between Ox particles and the other additives. Therefore, it leads to produce materials with a high density in Ox particles. Afterward, with this pressure the Ox particles are uniformly distributed along the PET nonwovens. Consequently, an enhancement in the surface compatibility/density of the composite was obtained, which will be an advance on the improvements of the mechanical behavior.

### 3.2. Morphological properties

The surface morphology of untreated and treated PET nonwoven was determined by SEM analysis, and the results are shown in **Fig. 1**. The original PET nonwoven exhibits a random network of overlapped fibers and multiple connected pores with a fairly smooth surface. From the PVDF coating process, the microstructure presented a continuous film structure with a thickness layer about few microns. Visible changes were observed after the fixation of PVDF/Ox, indicating that PET surface was totally covered by the PVDF/Ox particles. Regarding to the good dispersion of Ox onto PET fibers, it was supposed that a strong interfacial interactions between PET, PVDF and Ox are involved. By comparing the treated PET (i.e. PET-PVDF-ZnO, PET-PVDF-SiO<sub>2</sub> and PET-PVDF-TiO<sub>2</sub>), SEM images of PET-PVDF-TiO<sub>2</sub> showed an uniform distribution with high particles density at the fiber surface, resulted in a much smoother surface structure and the formation of bulkier aggregates of much smaller particles. This fact can be explained in terms of strong interaction between PET:PVDF-Ox, particularly for PET-PVDF-TiO<sub>2</sub>, which promotes structure morphology with tailored surface.

..... (Figure.1) .....

On the other hand, optical microscopy confirmed this phenomenon by the preponderance of uniform aggregates film at the fiber surface (**Fig. S1**). Therefore, it appeared that both

PDFV-Ox and CT successfully covered the PET fiber, in agreement with FTIR analysis, contact angle and TGA analysis (discussed in the following parts).

Wettability and diffusion resistance are of great importance to evaluate nonwovens for environmental application. The contact angle and capillarity of the fiber surface were investigated and the results are reported in **Fig.2**. As seen, the water contact angle of original PET, PET-PVDF-SiO<sub>2</sub>-CT, PET-PVDF-ZnO-CT and PET-PVDF-TiO<sub>2</sub>-CT are 1.97, 110.20, 120.41, and 111.20, respectively. This result indicated that modified PET nonwoven was more hydrophobic than pristine PET. Herein, nonwovens with good hydrophobicity would be beneficial not only for the improvement of mechanical and fire retardancy properties, but also the durability. Deeper insights in the changes of the apparent contact angles with time were investigated, and the results are summarized in **table. 1**. According to the obtained results, it was found that PET-PVDF is very hydrophobic materials, as compared to the other samples. Even, during 1 hour, the water cannot penetrate in PET-PVDF-Ox-CT samples, due to the high hydrophobicity of PVDF and the lotus effect. In our case, some unsaturated atoms like F, Ti, Si and Zn can decrease this hyper hydrophobicity, as supported by the measurements on the contact angle. Herein, the role of chitosan was to ensure the crosslink between unsaturated atoms and hydroxyl groups from chitosan. Thus the hydrophobicity was slightly increased by the CT grafting. This was confirmed by the droplet volume and the contact angle values, which were unchanged in time. By contrast, Ox is hydrophilic materials and hence the water could penetrate on the surface in less than 3 s (**table S3**).

..... (**Figure.2**) .....

..... (**Table.1**) .....

### 3.3. Structural properties

**Figure 3** and **figure S5** showed the XRD patterns of pure PET, PET-PVDF-SiO<sub>2</sub>-CT, PET-PVDF-TiO<sub>2</sub>-CT and PET-PVDF-ZnO-CT composites. These patterns were recorded to

analyze the structure and crystalline phase of prepared oxides. The broad diffraction band observed at  $18^\circ$  and  $25^\circ$  was attributed to the amorphous nature of the Ox. According to the JCPDS no 29-0085 and literature, the XRD diffraction of PET-PVDF-SiO<sub>2</sub>-CT exhibits a broad peak centered at  $2\theta = 22^\circ$ . This peak is associated to the SiO<sub>2</sub> particles, which shows the successful addition of amorphous SiO<sub>2</sub> in the PET fibers [17]. For the PET-PVDF-TiO<sub>2</sub>-CT pattern, the broader peaks observed at  $36.8^\circ$  and  $60.9^\circ$  were due to the formation of TiO<sub>2</sub>. While, the main peak observed at  $2\theta = 44^\circ$  in the PET-PVDF-ZnO-CT pattern confirmed the presence of ZnO nanoparticles, according to JCPDS card no 04 0850 [50]. In addition, **figure 4** confirms the successful preparation of PET-PVDF-Ox-CT composites by EDX-XRF analysis, where elemental F, N, Si, Ti and Zn can be observed in the sample composition. The elemental F and N can be observed in all spectrum of PET-PVDF-Ox-CT, suggesting the presence of PVDF and CT in the materials. Elements of carbon and oxygen can also be observed in all EDX spectrums which demonstrated the presence of various functional groups in the composites structure.

..... (Figure.3) .....

..... (Figure.4) .....

### 3.4. Infrared analysis

Infrared studies were carried out to ascertain the purity and nature of the functional groups that exhibited on prepared composites. The FTIR spectra of original and modified PET nonwovens are shown in (Fig. 5 and Fig. S2). The structure of original nonwoven displayed some bands in the region  $1720-650\text{ cm}^{-1}$ , attributed to the stretching vibration of CH<sub>2</sub>, C=O, and aromatic C=C. The peak observed at  $3100\text{ cm}^{-1}$  was attributed to the stretching vibration C-H present in the polyester fibers. The broad absorption peaks at around  $3437$  and  $1456\text{ cm}^{-1}$  are attributed to stretching vibrations of OH groups corresponding to the adsorbed water molecules on the samples surface. After PVDF fixation, the bands obtained at  $869\text{ cm}^{-1}$  were

attributed to the vibrations of  $\nu\text{CF}_2$  for amorphous PVDF [19]. The chemical fixations of Ox were confirmed by the presences of new supplementary peaks at low wavenumber. The band observed at  $515\text{ cm}^{-1}$  is attributed to the Zn–O stretching vibration, indicating the characteristic band of pure ZnO [19]. In addition, the deposition of  $\text{SiO}_2$  particles were confirmed by the enlargement of the band at  $1100\text{ cm}^{-1}$  assigned to the stretching vibration of O–Si–O. Indeed, the impregnation of  $\text{TiO}_2$  particles was confirmed by the band at  $700\text{ cm}^{-1}$  assigned to the stretching vibration of Ti–O [20]. Chitosan grafting induced a shift of the  $\nu\text{CF}_2$  peaks from  $869\text{ cm}^{-1}$  to  $875\text{ cm}^{-1}$  which might be due to the restriction on the vibration by the interaction occurred between  $\text{TiO}_2$ , CT and  $\text{CF}_2$  groups [21]. The peak obtained at  $1625\text{ cm}^{-1}$  was assigned to the  $\text{NH}_2$  group bend scissoring, indicating that chitosan were successfully coated the modified PET fibers [22]. In addition, the band appeared at  $1420\text{ cm}^{-1}$  and  $1156\text{ cm}^{-1}$  were attributed to the OH bending of primary alcoholic group and to C–N stretch in chitosan, respectively. From the FT-IR results, it can be summarized that CT, PVDF and Ox are correctly attached to PET. We estimated that the grafting occurs through the interaction of amine groups ( $-\text{NH}_2$ ) and hydroxyl groups ( $-\text{OH}$ ) through hydrogen bonding, which was in good agreement with hypothesis presented in the literature [23, 24].

Interestingly, the grafting of PVDF showed a characteristic peak appeared at  $1108\text{ cm}^{-1}$  and assigned to the stretching vibration of the C–O–C band of PVDF. This peak was disappeared for both PET-PVDF- $\text{TiO}_2$  and PET-PVDF- $\text{TiO}_2$ -PPT-CT modified nonwovens. This is due to effective chemical grafting of PVDF, which involved specific interaction between C–F<sub>2</sub> in PVDF and  $\text{TiO}_2$ /CT. Deeper insights in the IR spectra of PET-PVDF- $\text{TiO}_2$  and PET-PVDF- $\text{TiO}_2$ -CT revealed a markedly decreases in the peaks intensity which provides significant evidence of the additional functional groups from the additives. The latter should confirm the good compatibility between PVDF and  $\text{TiO}_2$ -CT.

..... (Figure.5) .....

### 3.5. Thermogravimetric analysis

Thermogravimetric analysis was performed to provide onset temperature and analyze the thermal properties of the untreated PET and treated nonwovens composites. Under nitrogen atmosphere, all samples were heated from room temperature to 800 °C at 20 °C/min and the results are showed in **figure. 6** and **figure. S3-4**. As first overview, the sample presents one single step for decomposition. The composite starts to decompose at 180–200 °C, which was in good agreement with previous reports [25-27]. The primary mass loss at the range of 100-200 °C is assigned to the evaporation of adsorbed water and the later decomposition is ascribed to the depolymerization of both PVDF and CT as organic molecules. The weight loss registered for PET-PVDF-OM at the range of 300-400 °C, indicating the effect of Ox on the thermal properties (**Table S4**). Here, the initial decomposition temperature of PET, PET-PVDF-ZnO, PET-PVDF-TiO<sub>2</sub> and PET-PVDF-SiO<sub>2</sub> are 333°C, 335°C, 491°C and 480 °C, respectively. The high temperature at maximum weight loss rate can also be found for these hybrids and the solid residues PET-PVDF-ZnO, PET-PVDF-TiO<sub>2</sub> and PET-PVDF-SiO<sub>2</sub> at 600 °C are 66.3%, 65.8% and 84.5%, respectively, showing again their good thermal stability, particularly for PET-PVDF-TiO<sub>2</sub> which was another confirmation of the good dispersion of TiO<sub>2</sub> particles.

..... (**Figure.6**) .....

### 3.5. Mechanical properties

As discussed above, the thermal behaviors and hydrophilicity are studied, and it is important to investigate the mechanical behavior of the composites. The results of the stress–strain are shown in **Figure. 7**. It is clear that all functional composites displayed an enhancement on the tensile strengths. The highest tensile strengths are obtained for the composite PET-PVDF-Ox-CT, whereas the lowest values are registered for unmodified PET. Here, the tensile strengths depend manly on the functionalization process, which cause some favorable influence on the

mechanical properties. The tensile strength of the PET-PVDF-Ox-CT is close to 10.20 MPa, which is adequate for nonwovens application. The tensile strength was increased from 2.30, 8.93, 9.81 to 10.19 for PET, PET-PVDF-SiO<sub>2</sub>-CT, PET-PVD-ZnO-CT and PET-PVDF-TiO<sub>2</sub>-CT, respectively. By comparing the results obtained for different OM, the modification with TiO<sub>2</sub> particles represented the higher tensile strength, as compared to the ZnO and SiO<sub>2</sub>. This evidences the good dispersion and fixation of TiO<sub>2</sub> particles into fiber surface, which regenerate an improvement on the mechanical behaviors. Results are confirmed by the hydrophobicity and SEM analysis. Thus, it was found that addition of PVDF, Ox and CT enhanced highly the mechanical properties of the resulting composite. According to the data obtained from the mechanical test, the increase in the hardness can certainly be attributed to the surface compatibility and the presence of the reinforcement nanoparticles (**Table. 2**). In other words, the nano-size of both reinforcing particles and PVDF/CT increased the interfacial contact between the particles and the fiber, leading to hardness elevation. As seen, the as-synthesized PET-PVDF-Ox-CT composite sample displayed 70% higher strength than the pristine sample. Interestingly, Young's modulus a PET-PVDF-TiO<sub>2</sub>-CT composites demonstrates the higher resistance (154.19 MPa). It was found that addition of PVDF/TiO<sub>2</sub>/CT, Young's modulus increased, suggesting the reinforcing effects of TiO<sub>2</sub> were stronger than those of ZnO and SiO<sub>2</sub>, due to the large distribution of particle into fiber surface. In all of the cases, the incorporation of PVDF/Ox/CT resulted in an increase of the storage modulus for all composites. However, PET-PVDF-TiO<sub>2</sub>-CT showed the higher elastic stress (10.19 MPa) than the other counterparts, confirming again the significant performance of PVDF, TiO<sub>2</sub> and CT for PET functionalization.

Since the presence of PVDF on the surface of PET-PVDF-Ox-CT increases significantly the hydrophobicity, the formation of intermolecular bonding between PET and Ox-CT can facilitate the stress transfer, producing increases on the mechanical stress. These facts reflect

the role of PDVF, which was attributed to the interfacial adhesion of coupling agent that could transform the inorganic surface from hydrophilic to hydrophobic nature. Thus, PET-PVDF-Ox-CT composite provides a great improvement of mechanical properties.

..... (Figure.7) .....

..... (Table.2) .....

### 3.6. Role of PVDF and oxides on the mechanical properties

Direct impregnation of Ox on PET sample results in limited improvement of the Young Modulus. So, we estimated that besides on the above results, the Ox and CT as additives have a key role in the improvements of the mechanical properties. Here, chitosan played an interesting role not only for the mechanical properties reinforcement, but also to ensure and maintain the Ox at the surface fiber during the employments. In addition, the surface compatibility between all components was also responsible for the significantly enhanced mechanical properties. Regarding to the values registered for PET-PVDF-TiO<sub>2</sub>-CT, the mechanical properties should be closely dependent on the interaction between polymer matrix CT/PVDF and TiO<sub>2</sub>, which evidences the compatibility and link between the components. Hence, the air voids (AV) have a negative effect on the mechanical properties. In presence of PVDF, we observed a large difference between PET-PVDF-SiO<sub>2</sub>-CT, PET-PVDF-ZnO-CT and PET-PVDF-TiO<sub>2</sub>-CT is due to the changes on the amount of AV presented for each sample [28]. In addition, lots of microvoids were created on the outer surface during the fabrication process, whereas there are visible changes in the cross-section. Herein, the heating pressure was of great importance, which drastically decreases the AV. Thus, the differences between all composites are explained in term of the Ox density present on the fiber surface. Consequently, PET-PVDF-TiO<sub>2</sub>-CT presents the lower amount of AV, as high density of TiO<sub>2</sub> particles were immobilized, as compared to the other counterpart ZnO and SiO<sub>2</sub> (Scheme.2). Additionally, the differences in AV confirmed the strong interaction between

PVDF and Ox at the fiber interface, which generates the formation of air voids. Therefore, the improvement on the mechanical properties can be attributed the good surface compatibility PVDF/TiO<sub>2</sub>/CT elements, which reduce the AV formation during the fabrication, particularly for PET-PVDF-TiO<sub>2</sub>-CT.

..... (Scheme.2) .....

### 3.8. Effect of oxides on mechanical properties and proposed mechanism

TiO<sub>2</sub>, ZnO and SiO<sub>2</sub> oxides were used in this study to clearly identify the effect of metal on mechanical properties (Tables.3). Results demonstrate that all oxides increased mechanical properties. Particularly, TiO<sub>2</sub> appeared to be more effectively, as compared to the other Ox. This allows that Ti metal present a strong oxidation promoter while the parent metal had a good compatibility with the other additives like PVDF and CT. Thus, it is worth mentioning that composites containing TiO<sub>2</sub> are still interesting than or closes to that for ZnO and SiO<sub>2</sub>, in mechanical properties [29].

This indicates the high amount of TiO<sub>2</sub> loaded on PET fiber, which can be attributed to the texture parameters such as the surface area. This must involve strong interactions of the terminal OH groups from PET with titanium particles at the expense of PVDF-TiO<sub>2</sub>. Thereby, this was a clear evidence of the key role of Ox fixation, especially for VTiO<sub>2</sub> in composite stabilization. Consequently, the stabilization resulting by the addition of OM induced visible increases on the thermal and mechanical properties. However, the surprisingly higher thermal stability noticed for PET-PVDF-TiO<sub>2</sub>-CT must be due to a more pronounced chemisorption of heat inside TiO<sub>2</sub> protected by organic moiety (PVDF/CT). To clearly demonstrate the role of the metal, additional attempts were performed and supported by soil release test. Except for silica, the stains are disappeared for TiO<sub>2</sub> and ZnO. As seen, the stains are completely released for the TiO<sub>2</sub> metal oxide, confirming again the high capacity of titanium atoms to

promote not only the strong interactions with the surface nonwoven but also the good compatibility of the resulting composite.

As discussed above, PET-PVDF-TiO<sub>2</sub>-CT presents a significant improvement on the result obtained on the mechanical properties of PET-PVDF-TiO<sub>2</sub>-CT demonstrates a significant increase in tensile strength and yield strength. Contributions of these improvements were explained by the reinforcement induced from the addition of OM particles. This is due to grain dispersion eventually leading to the occurrence of potential load transfer. Herein the possible strengthening mechanisms related to the improvement on the mechanical properties was attributed to the high dispersion and dislocation strengthening, as evidenced by the decreases in AV and the thermal stability of PET-PVDF-TiO<sub>2</sub>-CT composites [30, 31].

.....(Table.3).....

### 3.7. Sustainable and wash fastness property

Since detachment of the additive elements from the PET nonwovens would reduce the mechanical, a good wash resistant property is one of the key criteria for our PET-PVDF-Ox-CT composites to be sustainable materials for practical applications. **Figure.8** showed the washing tests during three cycles. As seen, in washing process, no loss on the PET-PVDF-Ox-CT contents during the washing environment was observed. This demonstrates that Ox was strongly attached to PET even in washing bath. Moreover, the retained and trapped Ox inside the PVDF is satisfying for further washings to achieve durability may be up to three more cycles. In addition, PET-PVDF-TiO<sub>2</sub> and PET-PVDF-ZnO-CT were tested after wash resistance, and the results show that no visible changes can be observed. This can be explained not only by the strong covalent bonds between the Ox, PVDF and CT, but also the good compatibility between these elements during the preparation of composite. Interestingly, with severe washing in the detergent solution, the Ox retained on composites, presumably due

to growth of Ox inside the construction and pores of nonwovens fiber, during the fixation and heating process. This was confirmed by SEM-EDX and FTIR analysis, indicating the presence of Ti and Zn metals after four washing cycles of PET-PVDF-ZnO-CT and PET-PVDF-TiO<sub>2</sub>-CT.

..... (Figure.8) .....

#### **4. Conclusions**

In this work, the influence of inorganic (TiO<sub>2</sub>, ZnO, SiO<sub>2</sub>) and organic (CT) moieties on the structure and mechanical properties of PET-PVDF/Ox/CT composite fiber was determined. SEM images revealed that oxides particles were well dispersed at the fiber surface. FT-IR analysis confirmed the good deposition of CT into PET-PVDF/Ox. DSC tests revealed the improvements on the thermal stability. It was found that tensile strength and strain of PET nonwovens were enhanced by PVDF/Ox/CT incorporation. The fixation of PVDF/Ox/CT into PET fibers strongly enhanced the tensile strength and thermal stability of obtained materials. The good durability of the prepared composite was confirmed by wash fastens test, indicating solid functional nonwovens against washing. The developed treatment method can be used in textile industry to produce functional nonwovens with high mechanical resistance. The study provides a reference for production and structure optimization and contributes to the design of modern fisheries equipment and engineering.

#### **ACKNOWLEDGEMENTS**

The authors would also like to thank Mr Christian Catel from ENSAIT/GEMTEX, France for his time and support in the preparation and characterization parts.

## REFERENCES

- [1] Zhu, Qiu-Hui, et al. "Comb-typed polycarboxylate superplasticizer equipped with hyperbranched polyamide teeth." *Colloids and Surfaces A: Physicochemical and Engineering Aspects* 553 (2018): 272-277.
- [2] Muthiah, Palanikkumar, Shu-Hau Hsu, and Wolfgang Sigmund. "Coaxially Electrospun PVDF– Teflon AF and Teflon AF– PVDF Core– Sheath Nanofiber Mats with Superhydrophobic Properties." *Langmuir*, 26.15 (2010): 12483-12487.
- [3] Plentz RS, Miotto M, Schneider EE, Forte M, Mauler RS, Nachtigall SMB. Effect of a macromolecular coupling agent on the properties of aluminum hydroxide/PP composites. *J Appl Polym Sci*, 101.3 (2006): 1799-1805.
- [4] Xie Y, Hill CAS, Xiao Z, Militz H, Mai C. Silane coupling agents used for natural fiber/polymer composites: a review. *Compos Appl Sci Manuf* 41.7 (2010): 806-819.
- [5] N. Bouazizi, F. Ajala, A. Bettaibi, M. Khelil, A. Benghnia, R. Bargougui, S. Louhichi, L. Labiadh, R. Benslama, B. Chaouachi, K. Khirouni, A. Houas, A. Azzouz, Metal-organo-zinc oxide materials: investigation on the structural, optical and electrical properties, *J. Alloys. Comp.* 656 (2016): 146-153.
- [6] WANG, Panpan, MA, Jun, WANG, Zhenghui, Enhanced separation performance of PVDF/PVP-g-MMT nanocomposite ultrafiltration membrane based on the NVP-grafted polymerization modification of montmorillonite (MMT). *Langmuir*, 28.10 (2012): 4776-4786.
- [7] Zhou, Jianfeng, et al. "Aminolysis of polyethylene terephthalate fabric by a method involving the gradual concentration of dilute ethylenediamine." *Colloids and Surfaces A: Physicochemical and Engineering Aspects* 513 (2017): 146-152.
- [8] K. Yao, J. Gong, J. Zheng, L. Wang, H. Tan, G. Zhang, Y. Lin, H. Na, X. Chen, X. Wen, Catalytic carbonization of chlorinated poly (vinyl chloride) microfibers into carbon microfibers with high performance in the photodegradation of Congo Red, *J. Phys. Chem. C.* 117.33 (2013): 17016-17023.
- [9] Niakan, Mahsa, Zahra Asadi, and Majid Masteri-Farahani. "A covalently anchored Pd (II)-Schiff base complex over a modified surface of mesoporous silica SBA-16: an efficient and reusable catalyst for the Heck-Mizoroki coupling reaction in water." *Colloids and Surfaces A: Physicochemical and Engineering Aspects* 551 (2018): 117-127.
- [10] H. Parangusan, D. Ponnamma, M.A. AlMaadeed, Flexible tri-layer piezoelectric nanogenerator based on PVDF-HFP/Ni-doped ZnO nanocomposites, *RSC Adv.* 7.79 (2017): 50156-50165.
- [11] X. Guan, Y. Zhang, H. Li, J. Ou, PZT/PVDF composites doped with carbon nanotubes, *Sens. Actuators A: Phys.* 194 (2013): 228-231..
- [12] Huang P, Cao M, Liu Q. Adsorption of chitosan on chalcopyrite and galena from aqueous suspensions. *Colloids Surf A Physicochem Eng Aspects.* 409 (2012): 167-175
- [13] Huang P, Cao M, Liu Q. Using chitosan as a selective depressant in the differential flotation of Cu–Pb sulfides. *Int J Miner Process* 106 (2012): 8-15.
- [14] J. Li, Y. Gong, N. Zhao, Preparation of N-butyl chitosan and study of its physical and biological properties, *J. Appl. Polym. Sci.* 98.3 (2005): 1016-1024.
- [15] V.R. Giri Dev, R. Neelkandan, N. Sudha, O.L. Shamugasundaram, R.N. Nadaraj, Chitosan- a polymer with wider applications, *Text. Mag.* 45.5 (2009): 1337-1348.
- [25] C.M. Costa, M.M. Silva, S. Lanceros-Mendez, Battery separators based on vinylidene fluoride (VDF) polymers and copolymers for lithium ion battery applications, *RSC Adv.* 3.29 (2013): 11404-11417.
- [16]. Takke, V., et al., Studies on the atmospheric air–plasma treatment of PET (polyethylene terephthalate) woven fabrics: effect of process parameters and of aging. *Journal of applied polymer science*, 114.1 (2009): 348-357.

- [17] Ahmed, H. B.; Emam, H. E., *Layer by Layer Assembly of Nanosilver for High Performance Cotton Fabrics. Fiber Polym.* 17.3 (2016): 418-426.
- [17] Emam, H. E.; Rehan, M.; Mashaly, H. M.; Ahmed, H. B., *Large Scaled Strategy for Natural/Synthetic Fabrics Functionalization via Immediate Assembly of AgNPs. Dyes Pigm.* 133 (2016): 173-183.
- [19] Bachan, Neena., "A Comparative Investigation on the Structural, Optical and Electrical Properties of SiO<sub>2</sub>-Fe<sub>3</sub>O<sub>4</sub> Core-Shell Nanostructures with Their Single Components." *Acta Metallurgica Sinica*, 28.11 (2015): 1317-1325.
- [20] Fayaz Ali, Sher Bahadar Khan, Tahseen Kamal, Khalid A. Alamry, Esraa M. Bakhsh, Abdullah M. Asiri, Tariq R.A. Sobahi, *Synthesis and characterization of metal nanoparticles templated chitosan-SiO<sub>2</sub> catalyst for the reduction of nitrophenols and dyes, Carbohydrate Polymers*, 192 (2018): 217-230.
- [21] S. Ganesan, B. Muthuraaman, V. Mathew, M.K. Vadivel, P. Maruthamuthu, M. Ashokkumar, S.A. Suthanthiraraj, *Influence of 2,6 (N-pyrazolyl)isonicotinic acid on the photovoltaic properties of a dye-sensitized solar cell fabricated using poly(vinylidene fluoride) blended with poly(ethylene oxide) polymer electrolyte, Electrochim. Acta*, 56.24 (2011): 8811-8817.
- [22] A.K. Tripathi, M.K. Singh, M.C. Mathpal, S.K. Mishra, A. Agarwal, *Study of structural transformation in TiO<sub>2</sub> nanoparticles and its optical properties, J. Alloy. Compd*, 549 (2013): 114-120.
- [23] Q. Zhou, X.P. Lei, J.H. Li, B.F. Yan, Q.Q. Zhang, *Antifouling, adsorption and reversible flux properties of zwitterionic grafted PVDF membrane prepared via physisorbed free radical polymerization, Desalination*, 337 (2014): 6-15.
- [24] Coates J *Encyclopedia of analytical chemistry. In: Meyers RA (ed) Interpretation of infrared spectra, a practical approach. Wiley, Chichester*, 21.4 (2007): 828-834.
- [25] Zhang L, Zhu X, Sun H, Chi G, Xu J, Sun Y *Control synthesis of magnetic Fe<sub>3</sub>O<sub>4</sub>-chitosan nanoparticles under UV irradiation in aqueous system. Curr Appl Phys*, 10.3 (2010): 828-833.
- [26] Ma W, Ya F, Han M, Wang R *Characteristics of equilibrium, kinetics studies for adsorption of fluoride on magnetic-chitosan particle. J Hazard Mater*, 143.1-2 (2007): 296-302.
- [27] Catauro, Michelina, et al. "Synthesis and chemical characterization of new silica polyethylene glycol hybrid nanocomposite materials for controlled drug delivery." *Journal of Drug Delivery Science and Technology* 24.4 (2014): 320-325.
- [28] Chiang C-L, Hsu S-W. *Synthesis, characterization and thermal properties of novel epoxy/expandable graphite composites. Polym Int*, 59.1 (2010): 119-126.
- [29] Suhailath, K., & Ramesan, M. T. *Investigations on the structural, mechanical, thermal, and electrical properties of Ce-doped TiO<sub>2</sub>/poly (n-butyl methacrylate) nanocomposites. Journal of Thermal Analysis and Calorimetry*, (2019): 1-11.
- [30] Kashiwagi, Takashi, et al. "Flammability properties of polymer nanocomposites with single-walled carbon nanotubes: effects of nanotube dispersion and concentration." *Polymer*, 46.2 (2005): 471-481.
- [31] Kashiwagi, Takashi, et al. "Nanoparticle networks reduce the flammability of polymer nanocomposites." *Nature materials*, 4.12 (2005): 928.

## List of Figures

---

**Scheme.1:** Schematic illustration of the synthetic procedure for PET-PVDF-Ox-CT composites.

**Scheme.2:** Reaction mechanism described the surface compatibility and microvoids of PVDF/MO<sub>x</sub>/CT of (a) PET-PVDF-TiO<sub>2</sub>-CT, (c) PET-PVDF-ZnO-CT and (d) PET-PVDF-SiO<sub>2</sub>-CT.

**Figure.1:** SEM micrograph of (a) Original PET, (b) PET-CT, (c) PET-PVDF, (d) PET-PVDF-ZnO-CT, (e) PET-PVDF-TiO<sub>2</sub>-CT and (f) PET-PVDF-SiO<sub>2</sub>-CT composites.

**Figure . 2:** Photograph of colored water immersion-height during 60 min and changes in drop shape of (a) PET, (b) PET-PVDF-SiO<sub>2</sub>-CT, (c) PET-PVDF-TiO<sub>2</sub>-CT and (d) PET-PVDF-ZnO-CT composites.

**Figure. 3:** XRD pattern of (a) PET, (b) PET-PVDF-SiO<sub>2</sub>-CT, (c) PET-PVDF-TiO<sub>2</sub>-CT and (d) PET-PVDF-ZnO-CT composites.

**Figure. 4:** ED-XRF spectra of (a) PET-PVDF-TiO<sub>2</sub>-CT, (b) PET-PVDF-ZnO-CT and (c) PET-PVDF-SiO<sub>2</sub>-CT.

**Figure. 5:** FTIR spectra of (a) PET, (b) PET-PVDF-SiO<sub>2</sub>-CT, (c) PET-PVDF-TiO<sub>2</sub>-CT and (d) PET-PVDF-ZnO-CT composites.

**Figure. 6:** TGA patterns of (a) PET, (b) PET-PVDF-ZnO-CT, (c) PET-PVDF-SiO<sub>2</sub>-CT and (d) PET-PVDF-TiO<sub>2</sub>-CT composites.

**Figure. 7:** Stress–strain curves of (a) Original PET, (b) PET-PVDF-SiO<sub>2</sub>-CT, (c) PET-PVDF-ZnO-CT and (d) PET-PVDF-TiO<sub>2</sub>-CT composites

**Figure.8:** Releases of oil droplet after washing during 60 min for (a) PET, (b) PET-PVDF-ZnO-CT, (c) PET-PVDF-TiO<sub>2</sub>-CT and (d) PET-PVDF-SiO<sub>2</sub>-CT.

## List of tables

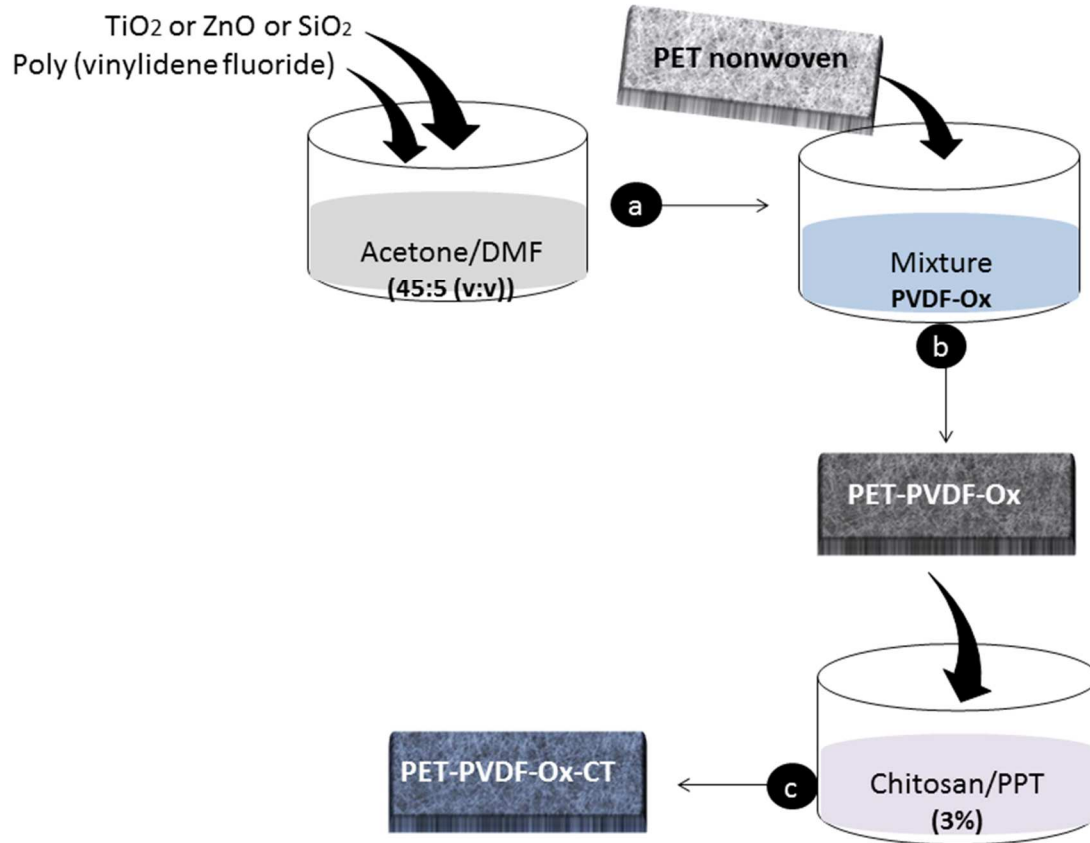
---

**Table.1:** Evolution in time of the contact angle for PET and modified counterparts.

**Table.2:** Young's (E) modulus and the elastic stress ( $\sigma$ ) values for original and treated PET nonwovens

**Table.3:** Main features in mechanical test of PET and its modified counterparts.

**Scheme.1**



Scheme.2

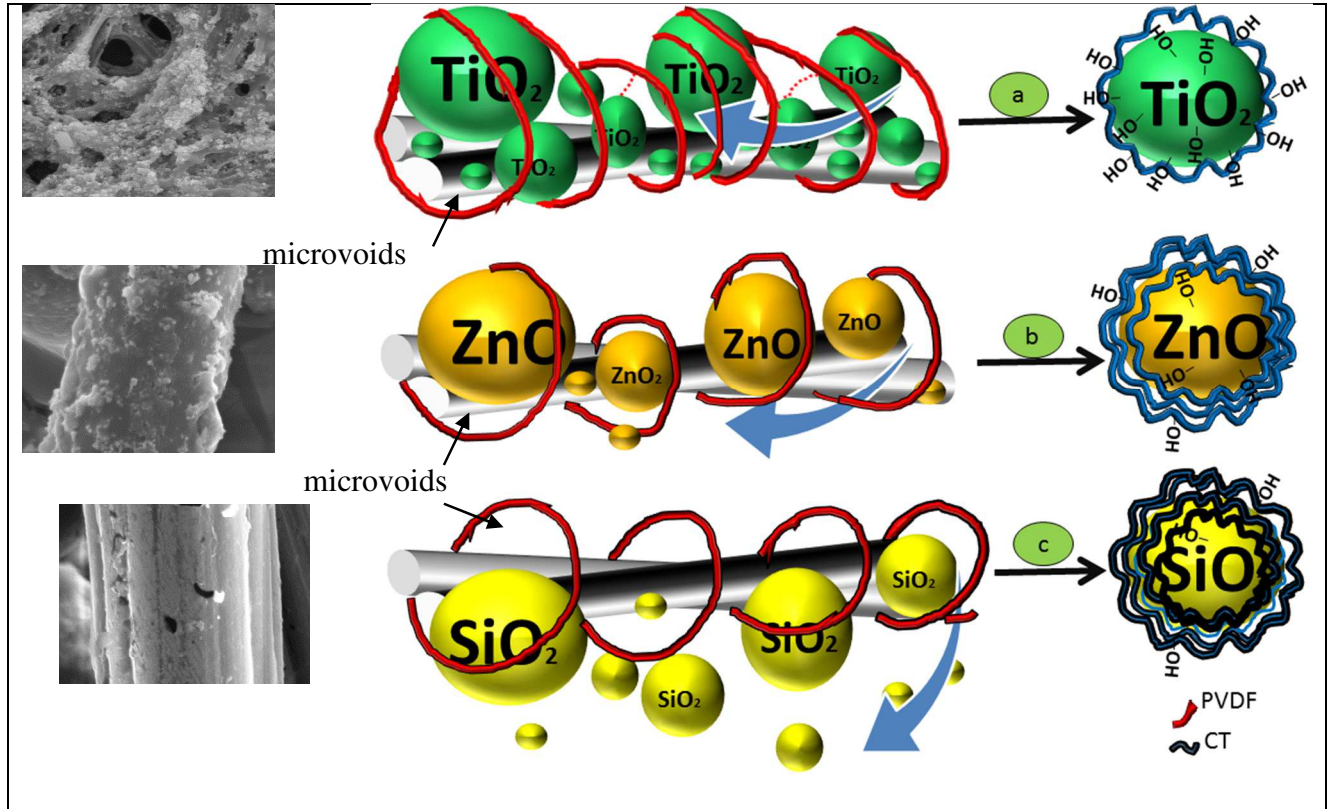


Figure.1

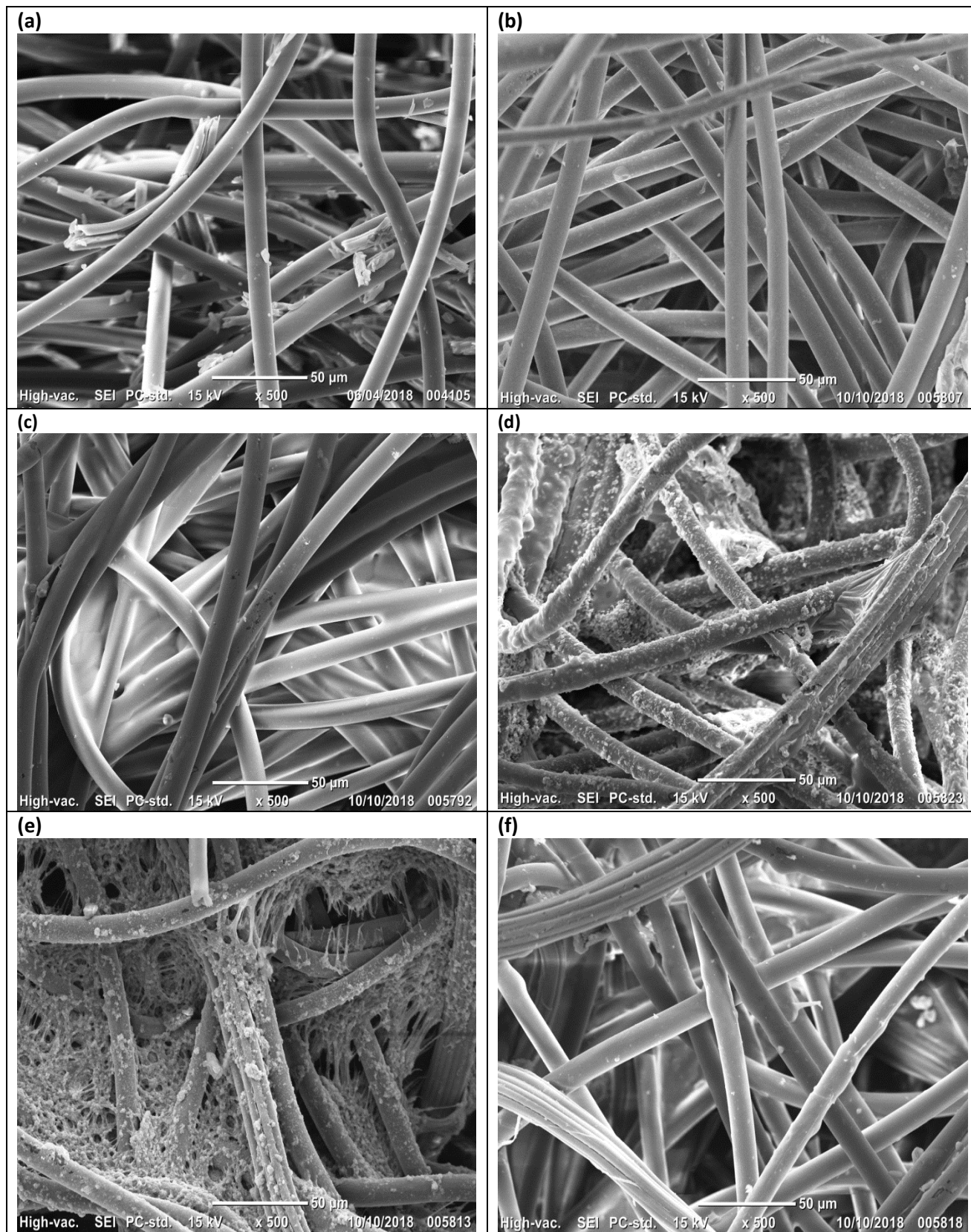


Figure.2

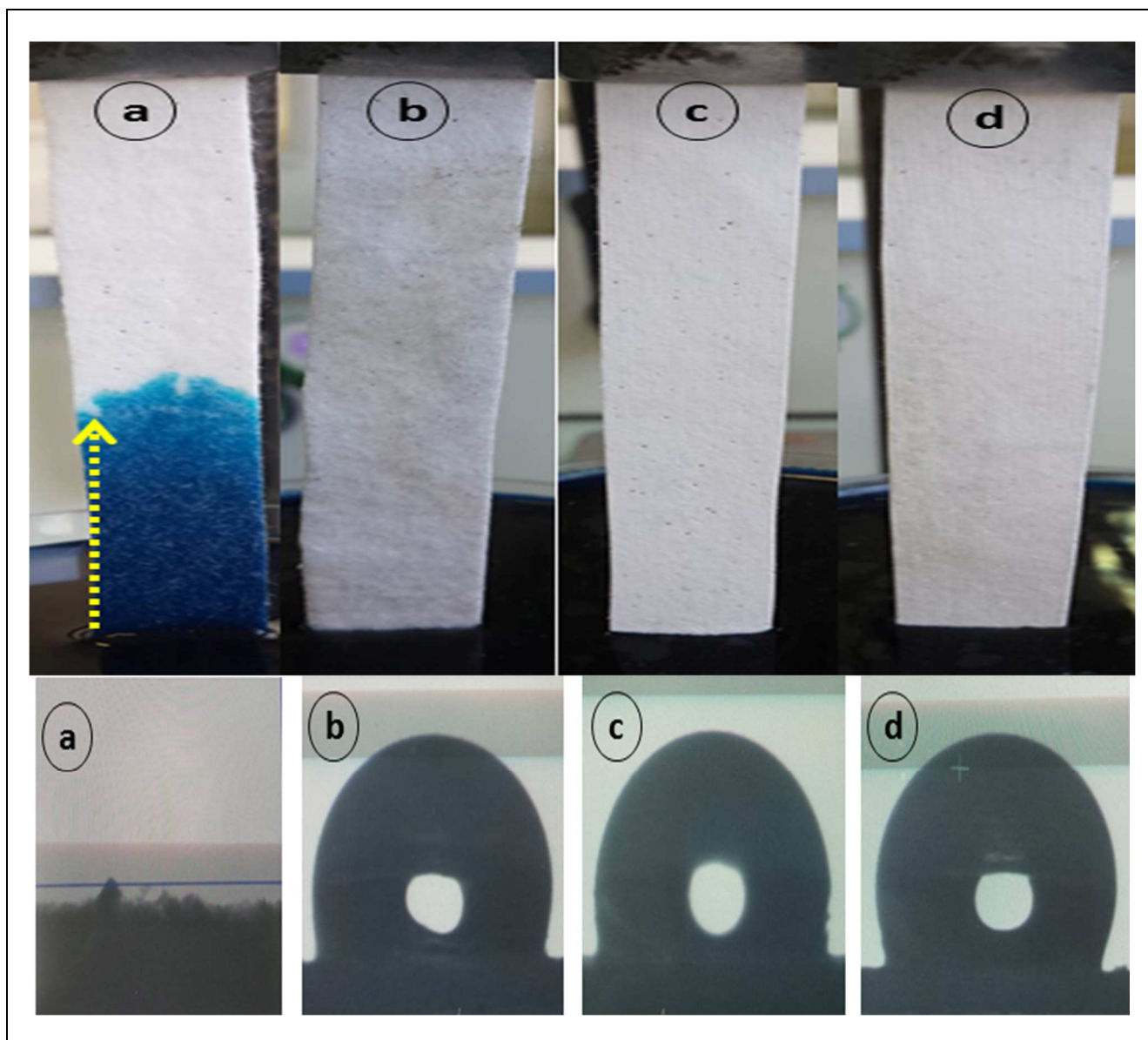


Figure.3

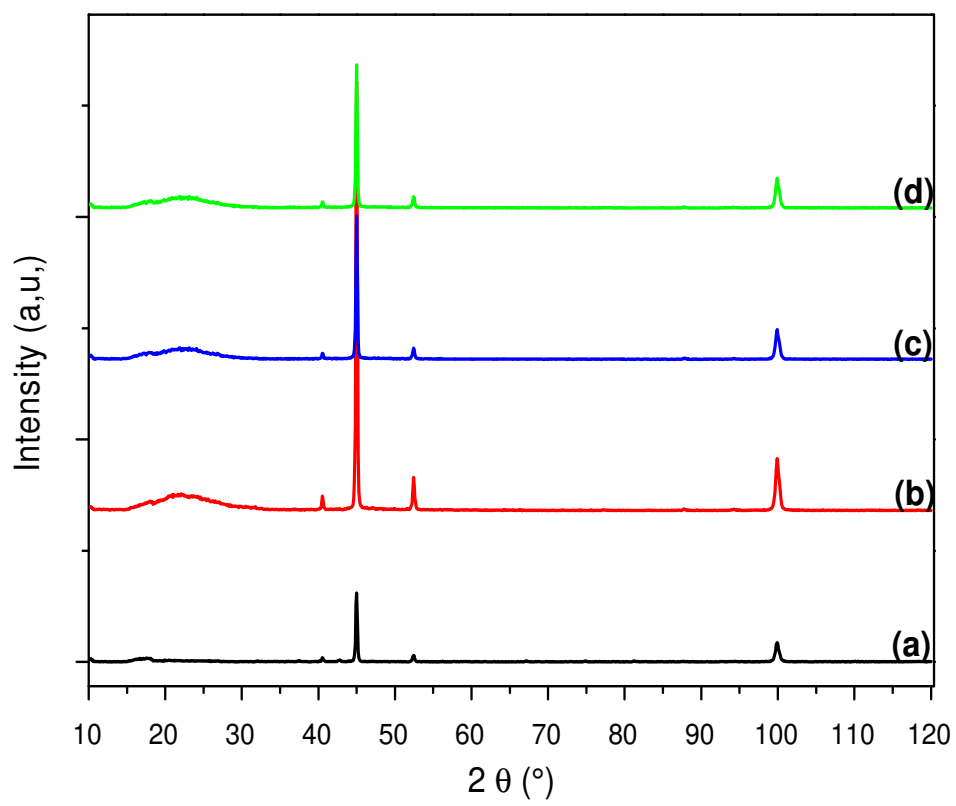
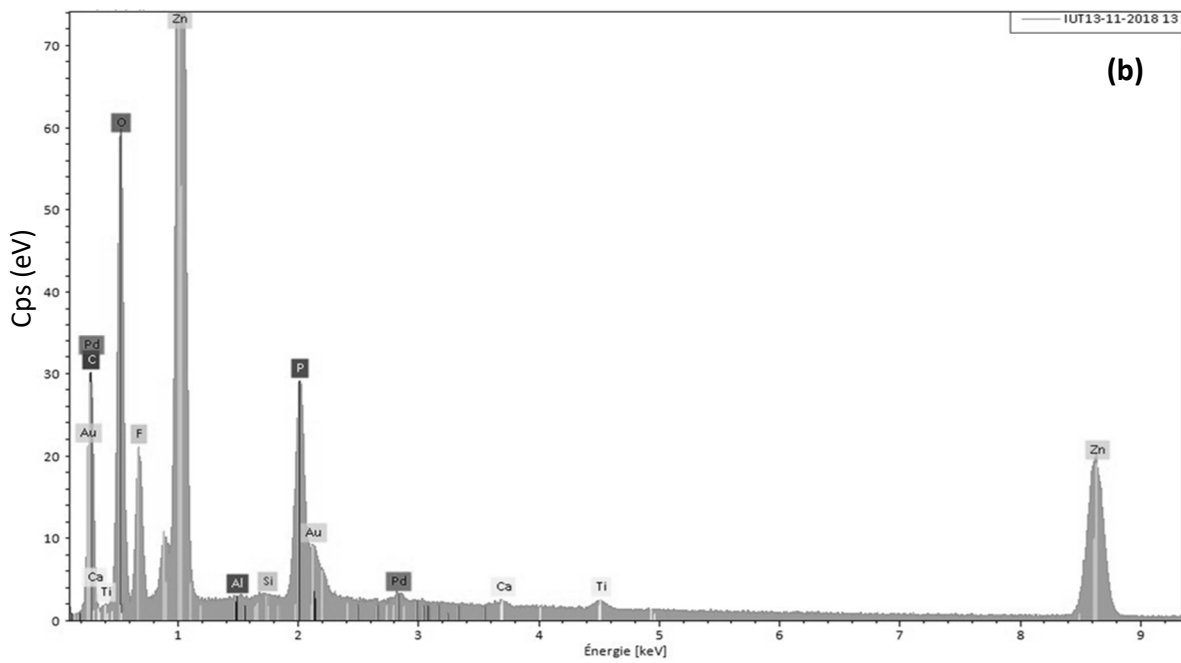
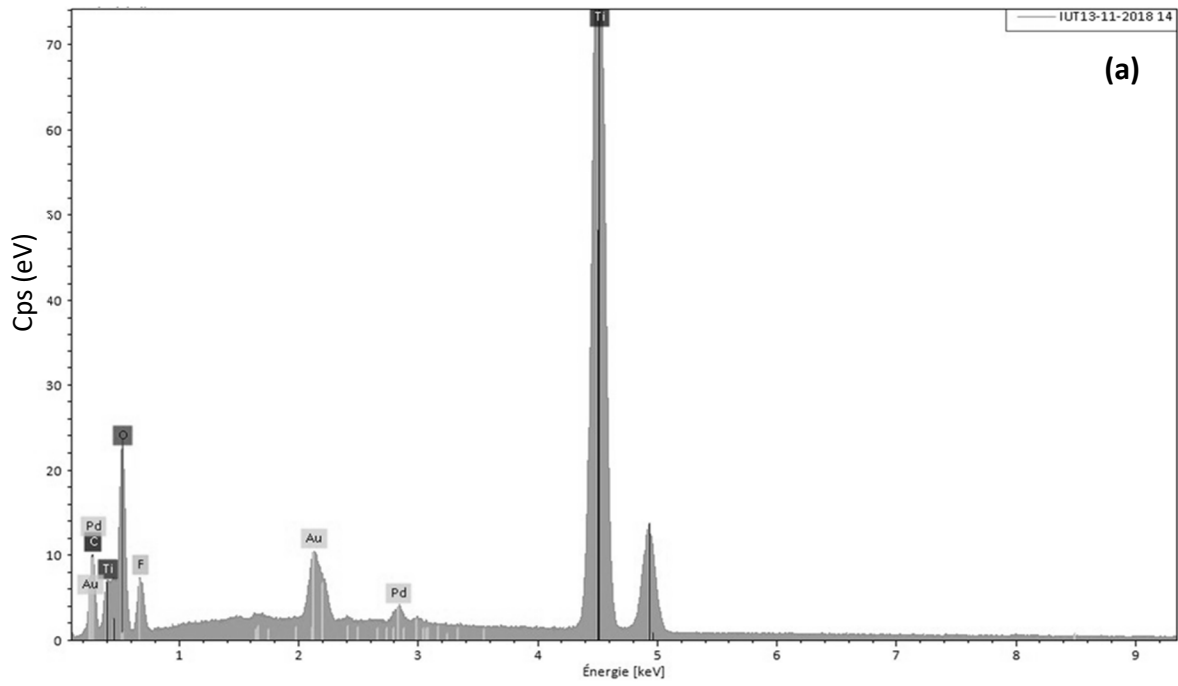


Figure.4



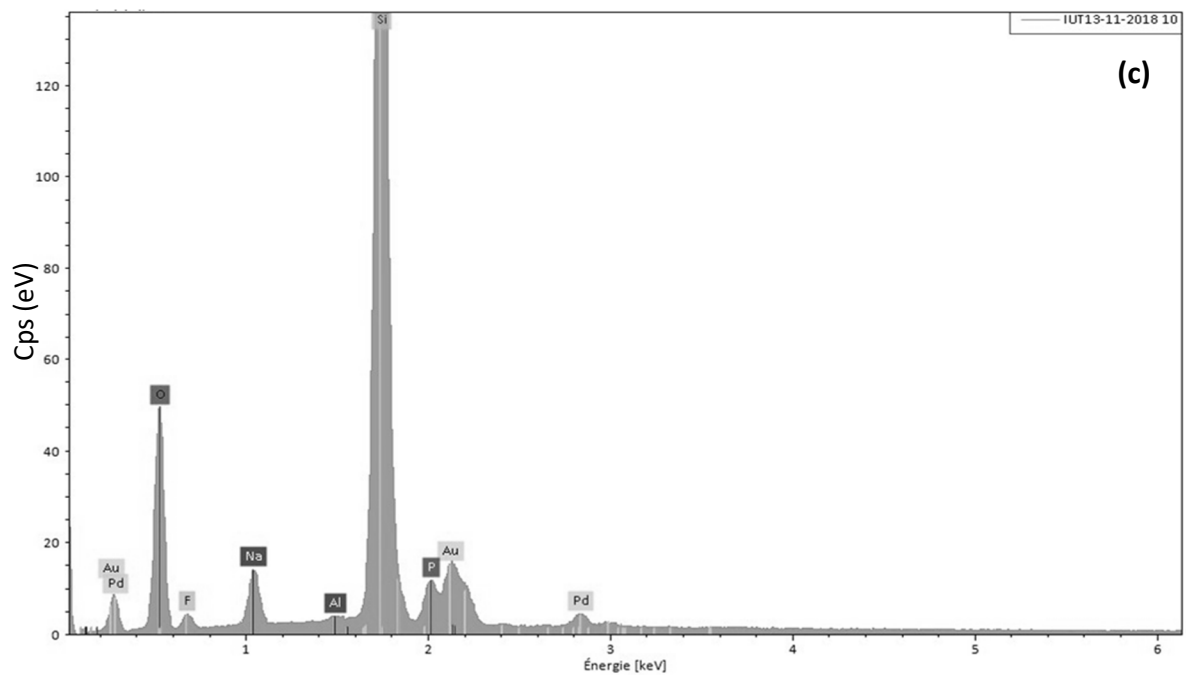
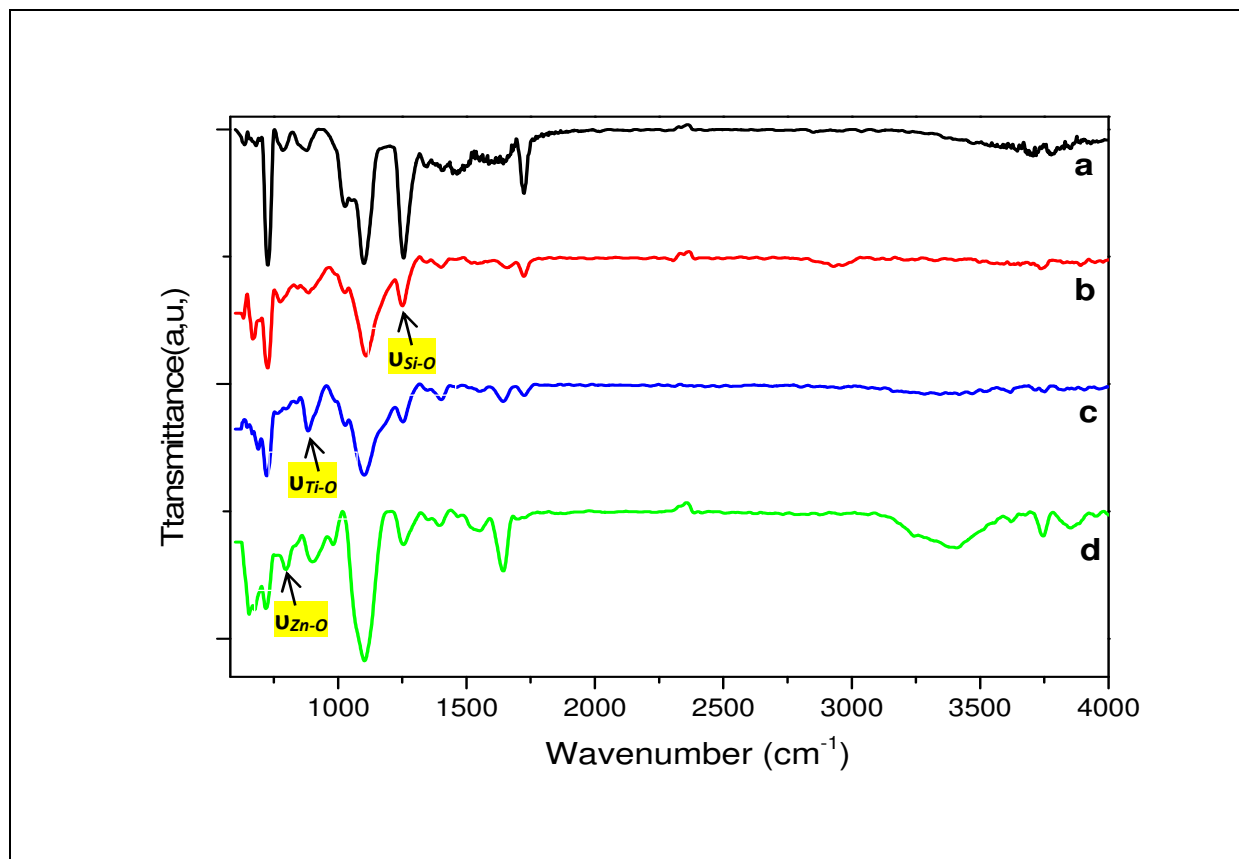
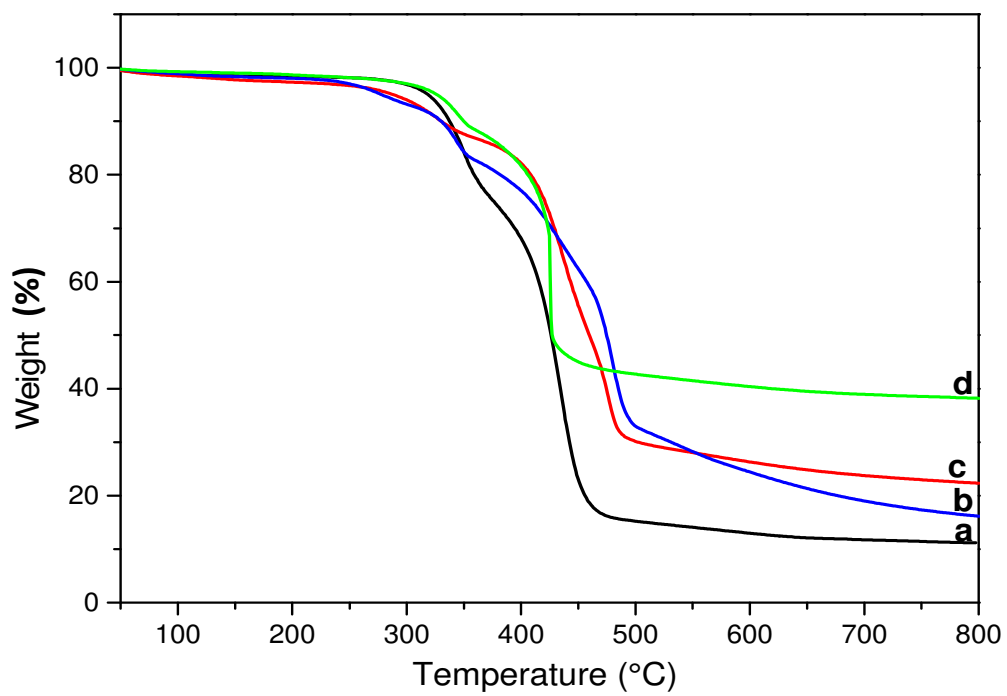


Figure.5



**Figure.6**



**Figure.7**

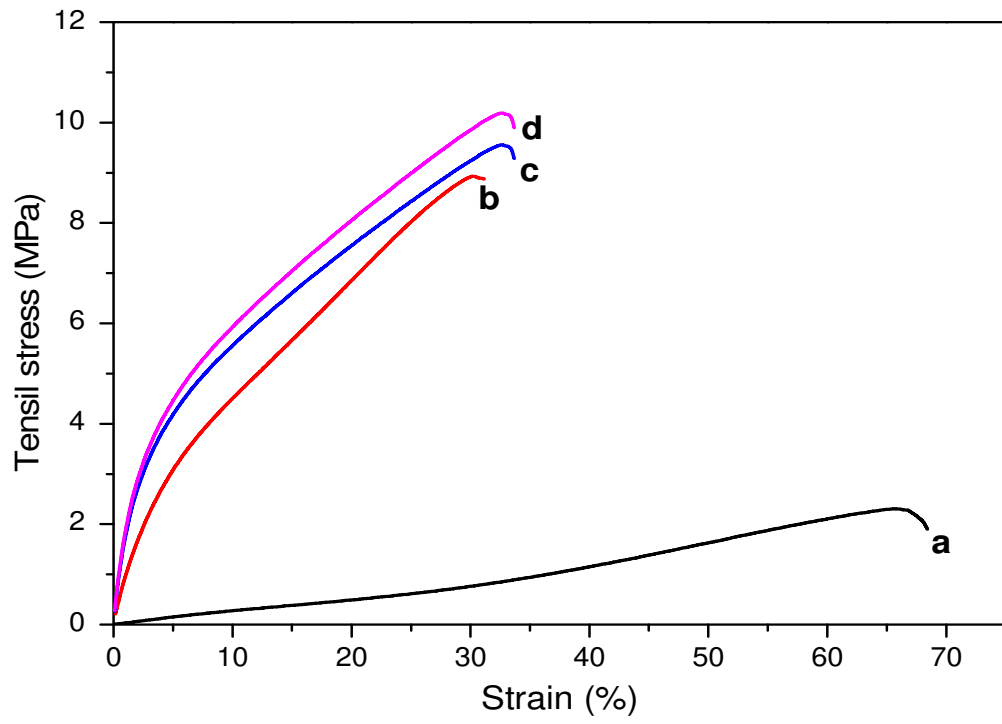
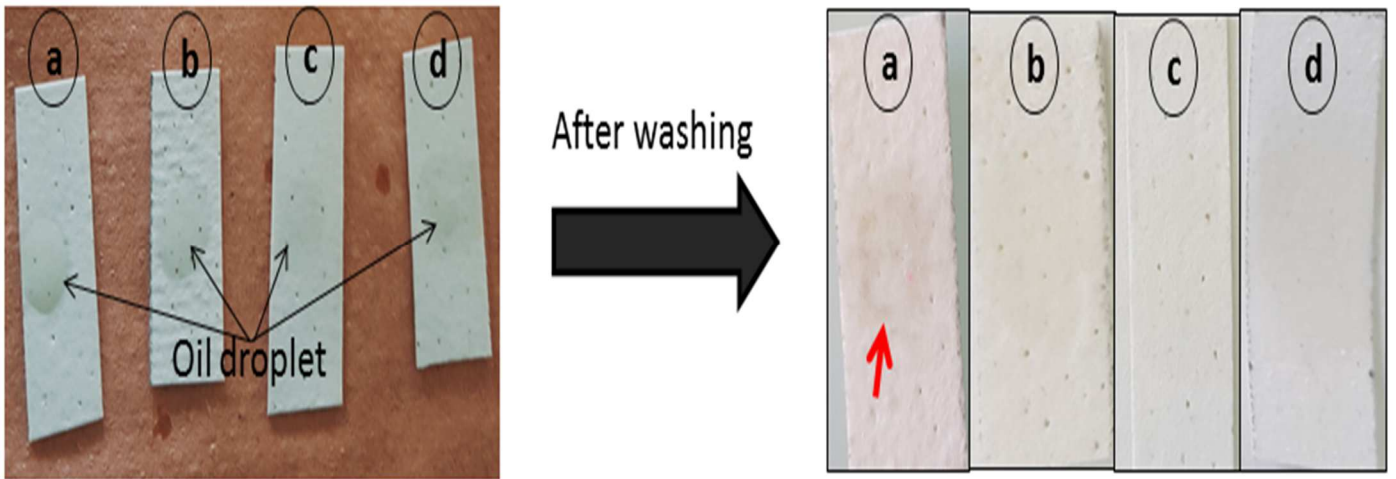


**Figure.8**



No releases of particles

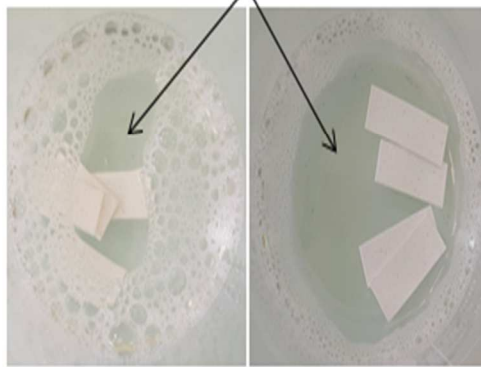


**Table.1**

Samples	Contact angle $\Theta$ (°)			
	1 min	5 min	30 min	60 min
PET	2	0	0	0
PET-PVDF-SiO <sub>2</sub> -CT	110	110	108	103
PET-PVDF-ZnO -CT	120	115	114	114
PET-PVDF-TiO <sub>2</sub> -CT	111	109	105	101

**Table.2**

<b>Samples</b>	<b><math>\sigma^*</math> (MPa)</b>	<b><math>E^*</math> (MPa)</b>
PET	2.30	0.50
PET- PVDF- SiO <sub>2</sub> -CT	8.93	73.00
PET- PVDF-ZnO-CT	9.81	127.00
PET- PVDF-TiO <sub>2</sub> -CT	10.19	154.00

\*  $\sigma$  and  $E$  where determined according to ISO 9073-3 norms.

**Table. 3**

<b>Samples</b>	<b><math>\sigma</math>(MPa)</b>	<b>E (MPa)</b>
PET	2.30	0.50
PET-PVDF	8.70	54.00
PET-CT	3.90	9.00
PET- SiO <sub>2</sub>	4.47	8.00
PET-PVDF-SiO <sub>2</sub>	9.66	18.00
PET-TiO <sub>2</sub>	11.40	27.00
PET-PVDF-TiO <sub>2</sub>	9.88	32.00
PET-ZnO	8.64	20.00
PET-PVDF-ZnO	9.44	24.00

# Graphical abstract

